

## Character of charge transfer excitons in $\text{Sr}_2\text{CuO}_2\text{Cl}_2$

A. S. Moskvin

*Department of Theoretical Physics, Ural State University, 620083 Ekaterinburg, Russia*

R. Neudert, M. Knupfer, J. Fink, and R. Hayn

*Institut für Festkörper- und Werkstofforschung (IFW) Dresden, D-01171 Dresden, Germany*

(Received 22 January 2002; published 2 May 2002)

High resolution electron energy loss spectroscopy (EELS) measurements of the insulating, layered cuprate compound  $\text{Sr}_2\text{CuO}_2\text{Cl}_2$  have been performed with a transferred momentum near  $\mathbf{k}=0$  and in a wide energy range up to 20 eV. To interpret the data a semiquantitative embedded cluster approach is applied to describe the electron-hole excitations in insulating cuprates. The theory includes the complete set of Cu  $3d$  and O  $2p$  orbitals and predicts a rather wide ( $2 \div 13$  eV) spectral range of the main dipole-allowed one- and two-center charge transfer (CT) transitions whose positions are in good quantitative agreement with the experimental spectra. Both, theory and the experimental data show that the CT gap is determined by a superposition of nearly degenerate one-center, localized CT excitations and two-center CT excitons with sizable dispersion.

DOI: 10.1103/PhysRevB.65.180512

PACS number(s): 74.72.Jt, 71.35.-y, 79.20.Uv

The nature of the electron-hole excitations in parent quasi-2D cuprates such as  $\text{La}_2\text{CuO}_4$ ,  $\text{Sr}_2\text{CuO}_2\text{Cl}_2$ ,  $\text{YBa}_2\text{Cu}_3\text{O}_6$ , and their 1D counterparts like  $\text{Sr}_2\text{CuO}_3$ ,  $\text{Sr}_2\text{CuO}_2$ ,  $\text{Li}_2\text{CuO}_2$  represents one of the most important, challenging issues both for the high  $T_c$  problem and, in general, for strongly correlated oxides. It is now believed that the most intense low-energy electron-hole excitations in insulating copper oxides correspond to the transfer of electrons from O to Cu in the  $\text{CuO}_2$  layer, hence these materials are charge transfer (CT) insulators.<sup>1</sup> However, there is much ambiguity concerning the nature of this spectral feature. Sometimes, only the intense band near 2 to 3 eV is connected with the O  $2p$  - Cu  $3d$  charge transfer, and higher-lying structures are assigned to Cu  $4s$ , Cu  $4d$ , Sr  $5d$  or La  $5d/4f$  states depending on the actual chemical structure. The band structure calculations, including LDA+U, fail to clarify the situation since they cannot reproduce the important effects of intra-atomic correlations which are important both for the ground and the excited state. Moreover, the electron-hole excitations of Mott insulators cannot be treated as independent excitations of single-particle states.

One of the most ideal model compounds of a 2D CT insulator is  $\text{Sr}_2\text{CuO}_2\text{Cl}_2$  on which we will concentrate the following discussion. Studying this compound using angle resolved photoemission spectroscopy (ARPES) it was found that the lowest excitation consists of a Zhang-Rice (ZR) singlet with a small dispersion of the order of  $2J$  ( $J$  being the in-plane exchange integral), i.e., with a high effective mass.<sup>2</sup> Different from ARPES where an electron is emitted, the excitations in electron energy-loss spectroscopy (EELS) represent electron-hole pairs. The first analysis<sup>3</sup> of excitons in  $\text{Sr}_2\text{CuO}_2\text{Cl}_2$  revealed a surprisingly large energy dispersion of about 1.5 eV along  $[110]$  which was interpreted in terms of a small exciton moving freely through the lattice without disturbing the antiferromagnetic spin background, in contrast to the single hole motion. This model of Zhang and Ng (ZN) is restricted to the Cu  $3d_{x^2-y^2}$  and O  $2p_\sigma$  orbitals and the elementary excitation consists of a  $\text{Cu}^+$  and a neighboring Zhang-Rice singlet-like excitation in Cu and O orbitals.<sup>4</sup> Al-

ready a shorthand inspection of the original experimental data,<sup>3</sup> and especially of the high-resolution EELS spectra<sup>5</sup> for this system point to some essential shortcomings of the ZN-model. In particular, the nature of several dispersionless narrow bands (one of them with a small binding energy of only about 2 eV) is not explained. Moreover, the high-resolution measurements reveal a very rich multi-excitonic nature of the EELS spectra.

In order to get a better experimental basis of electron-hole excitations in  $\text{Sr}_2\text{CuO}_2\text{Cl}_2$  we present here high resolution EELS data in a wide energy range up to 20 eV and not restricted to 8 eV as in Refs. 3 and 5. We limit ourselves to a momentum transfer near zero where only dipole allowed transitions are visible. For its interpretation an embedded cluster method is applied which extends the ZN-theory with respect to two points. It includes the complete set of Cu  $3d$  and O  $2p$  orbitals of the  $\text{CuO}_4$  plaquette and it distinguishes two types of excitons, namely localized one-center excitations and two-center excitons extending over two  $\text{CuO}_4$  plaquettes.

For the EELS measurements, films of about 100 nm thickness were cut from a  $\text{Sr}_2\text{CuO}_2\text{Cl}_2$  single crystal using an ultramicrotome equipped with a diamond knife. EELS spectra were recorded in transmission using a spectrometer described in detail elsewhere.<sup>6</sup> The energy and momentum resolution were chosen to be 115 meV and  $0.05 \text{ \AA}^{-1}$ , respectively. Prior to the measurements, the crystal structure and the orientation of the films were characterized by electron diffraction.

In Fig. 1 we show the imaginary part of the dielectric function,  $\epsilon_2$ , for a small momentum transfer in the a-b plane of  $0.1 \text{ \AA}^{-1}$  which corresponds to the optical limit. The dielectric function has been derived from the measured loss function via a Kramers-Kronig analysis. Also shown in Fig. 1 is an assignment of the individual features in  $\epsilon_2$  which will be presented in detail below.

To analyze the data we apply the embedded molecular cluster method. It is an effective method to describe excitonic states in strongly correlated Mott-Hubbard insulators

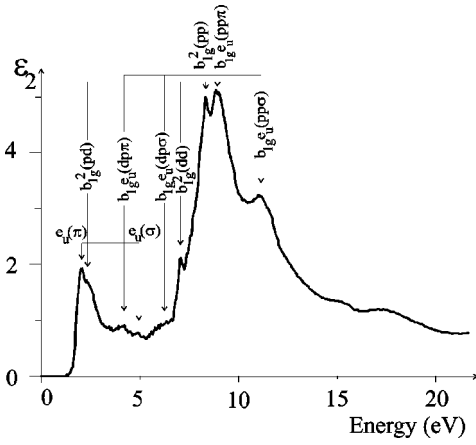


FIG. 1. The spectral dependence of the imaginary part of dielectric function  $\epsilon_2(\omega)$  for  $\text{Sr}_2\text{CuO}_2\text{Cl}_2$ . Arrows mark the predicted energy position of one-center, two-center  $b_{1g}^b$  channel, and  $b_{1g}e_u$  channel CT transitions.

especially with small effective electron-hole separation. In the present context we use one or two neighboring  $\text{CuO}_4$  plaquettes embedded into the  $\text{CuO}_2$  plane.

*One-center excitons.* Beginning from 5 Cu  $3d$  and 12 O  $2p$  atomic orbitals for a  $\text{CuO}_4$  cluster with  $D_{4h}$  symmetry, it is straightforward to form 17 symmetrized even  $a_{1g}$ ,  $a_{2g}$ ,  $b_{1g}$ ,  $b_{2g}$ ,  $e_g$  and odd  $a_{2u}$ ,  $b_{2u}$ ,  $e_u(\sigma)$ ,  $e_u(\pi)$  orbitals. The even Cu  $3d$   $a_{1g}$  ( $3d_{z^2}$ ),  $b_{1g}$  ( $3d_{x^2-y^2}$ ),  $b_{2g}$  ( $3d_{xy}$ ), and  $e_g$  ( $3d_{xz}$ ,  $3d_{yz}$ ) orbitals hybridize due to strong Cu  $3d$ -O  $2p$  covalency with the even O  $2p$  orbitals of the same symmetry, thus forming appropriate bonding  $\gamma^b$  and antibonding  $\gamma^a$  states.

Fig. 2 represents a realistic single-hole energy spectrum for a  $\text{CuO}_4$  plaquette embedded into an insulating cuprate like  $\text{Sr}_2\text{CuO}_2\text{Cl}_2$ . For illustration we show also a step-by-step formation of the cluster energy levels from the bare Cu  $3d$  and O  $2p$  levels with the successive inclusion of the crystalline field (CF) effects, the O  $2p$ -O  $2p$  and the Cu  $3d$ -O  $2p$  covalency. We used typical values for the differ-

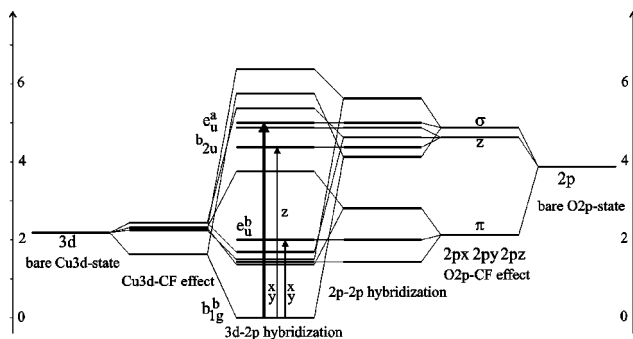


FIG. 2. Model single-hole energy spectra for a  $\text{CuO}_4$  plaquette based on simple cluster model with parameters relevant for  $\text{Sr}_2\text{CuO}_2\text{Cl}_2$  and a number of other insulating cuprates. Only the ground state and the nonbonding orbitals that are final states of dipole-allowed CT transitions are denoted and transitions marked by arrows. The other orbitals from bottom to top are given as  $b_{2g}^b$ ,  $a_{2g}$ ,  $a_{1g}^b$ ,  $e_g^b$ ,  $b_{2g}^a$ ,  $a_{2u}$ ,  $e_g^a$ ,  $b_{1g}^a$ , and  $a_{1g}^a$ .

ent energy parameters in accordance with several estimates in the literature that can be summarized as follows (in eV):  $\epsilon_p - \epsilon_d \approx 2-3$ ,  $\Delta_p = \epsilon_{p\sigma} - \epsilon_{p\pi} \approx 1-3$  ( $\epsilon_{p\pi} < \epsilon_{pz} < \epsilon_{p\sigma}$ ),  $t_{pd} \approx 1.0-1.5$ , and  $t_{pp\sigma} \approx 0.8$ ,  $-t_{pp\pi} \approx 0.2-0.4$ , where  $\epsilon_i$  denote on-site energies of the corresponding orbitals and  $t_i$  denote the special transfer integrals.<sup>7,8</sup> The energies  $\epsilon_d$  and  $\epsilon_p$  are the centers of gravity for the Cu  $3d$  and O  $2p$  manifolds, respectively.

Among the numerous one-center electron-hole CT excitations the first candidates for dipole-active excitons are CT transitions from the ground state  $b_{1g}^b$  to the purely oxygen doublet O  $2p_\pi$ -O  $2p_\sigma$  hybrid states  $e_u^{a,b}$ , which are allowed in “in-plane” polarization  $\vec{E} \perp C_4(x,y)$ . The transition to a purely oxygen O  $2p_z$ -like state  $b_{2u}$  is allowed in “out-of-plane” polarization  $\vec{E} \parallel C_4(z)$  which is however not measured in Fig. 1. The two excitations to  $e_u^b$  and  $e_u^a$  differ by the oxygen hole density distribution: the former has predominantly O  $2p_\pi$  character, while the latter is O  $2p_\sigma$  dominated. Discussing shortly the dipole inactive excitons one should note the  $a_{2g}$  excitation with purely oxygen O  $2p_\pi$  holes. In accordance with the model energy spectrum (see Fig. 2) its energy should be of the order of 1.5–1.8 eV, or in other words appears to be lower than the optical gap. This circumstance draws specific attention to this exciton, despite it is dipole forbidden.

Consequently, we predict two one-center excitons to be visible in the experimental spectra shown of Fig. 1: namely the  $e_u(\pi)$  and  $e_u(\sigma)$  excitons with predominantly  $2p_\pi$  and  $2p_\sigma$  orbital weight, respectively. Its energy separation and also its relative intensity are determined by the level of the  $p_\pi$ - $p_\sigma$  mixing characterized by the mixing angle  $\alpha_e \approx -(t_{pp\sigma} + t_{pp\pi})/\Delta_p$ . The respective one-center excitons may be represented rather simply as a hole rotating on the four nearest oxygens around an electron dominantly localized in the Cu  $3d_{x^2-y^2}$  state with a minimal electron-hole separation  $R_{eh} \approx R_{CuO} \approx 4$  a.u. [see Fig. 3(a)]. This low distance leads to a considerable Coulomb attraction such that we estimate the energy of the  $e_u(\pi)$  exciton to be about 2 eV. The final  $e_u(\pi)$  and  $e_u(\sigma)$  states are unstable with regard to the formation of Jahn-Teller (or pseudo-Jahn-Teller) centers with a resulting self-localization of the appropriate CT excitation. This effect is especially important for the  $e_u(\pi)$  exciton due to the predominantly O  $2p_\pi$  nature of the hole state resulting in small transfer integrals and relatively large effective mass for the exciton.

For the relative intensities of the  $e_u(\pi)$  and  $e_u(\sigma)$  excitons it is easy to obtain  $I[e_u(\pi)]/I[e_u(\sigma)] = \tan^2 \alpha_e$  with the mixing angle  $\alpha_e$ . We find this ratio to be about 0.1 resulting in small but nonzero intensity for the  $e_u(\pi)$  exciton. The high-energy  $e_u(\sigma)$  exciton is expected to manifest significant higher intensity both in optical and EELS spectra.

*Two-center excitons.* The local two-atomic O  $2p$ -Cu  $3d$  charge transfer generates not only intra-center excitations within one  $\text{CuO}_4$  plaquette but also inter-center excitons. These inter-center transitions between two  $\text{CuO}_4$  plaquettes may be considered as quanta of the disproportionation reaction



and two-center excitations. The one-center excitons provide small additional peaks on the dominant structures given by the two-center excitons.

Having positioned the lowest one- and two-center excitons, the higher states are fixed by the chosen parameter values (see Fig. 1). Remarkably, all the excitations which were analyzed before correspond to visible features in  $\epsilon_2$ . The highest intensity is found at about 9 eV and it is connected with the two-center excitons  $b_{2g}^2(pp)$  and  $b_{1g}e_u(pp\pi)$  of dominantly oxygen character. This shows that important spectral information is contained in the region above 8 eV. The highest excitation at about 12 eV is interpreted to be  $b_{1g}e_u(pp\sigma)$ , and then the spectral intensity decreases. The peak at about 18 eV is likely to be attributed to transitions with O  $2s$  initial state.

A close examination of other materials shows that the two-component structure of the CT gap appears to be a commonplace for many parent cuprates.<sup>13-15</sup> The dipole-allowed localized  $b_{1g} \rightarrow e_u^b$  excitation within the  $\text{CuO}_4$  plaquette related essentially to the  $e_u(\pi)$  state is distinctly seen in optical and EELS spectra for different insulating cuprates as a separate weak feature or a low-energy shoulder of the more intense band near 2.5 eV assigned to the inter-center CT transition associated with the Zhang-Rice singlet-like excitation  $b_{1g}^2(dp)$ .<sup>9</sup> The small intensity of the one-center  $e_u(\pi)$  exciton is explained by the dominantly O  $2p_\pi$  nature of the final state and by the strong tendency to self-localization (trapping).

One may wonder why such a double-peak structure of the lowest excitation is not seen in the corresponding ARPES spectra of  $\text{Sr}_2\text{CuO}_2\text{Cl}_2$ . There, the lowest excitation is clearly

connected with the ZR-quasiparticle,<sup>2</sup> and the nonbonding oxygen  $p_\pi$  orbitals appear with 1.5 eV higher binding energy (see Refs. 8 and 10). The reason is that EELS (or optical absorption) creates electron-hole pairs and the smaller extent of the one-center exciton leads to a Coulomb contribution to the exciton binding energy which compensates the ZR-singlet binding energy. On the other hand, comparing the different two-center excitons, the energy difference between ZR-singlet and nonbonding oxygens is seen in the difference between  $b_{1g}^2(pd)$  and  $b_{1g}e_u(dp\pi)$  (roughly 1.7 eV in Fig. 1).

In conclusion, we measured and interpreted the electron-hole excitations of  $\text{Sr}_2\text{CuO}_2\text{Cl}_2$ . We extended the Zhang-Ng model by considering the complete set of Cu  $3d$  and O  $2p$  orbitals and by introducing one-center and two-center excitons. Instead of one  $d-p_\sigma$  CT transition of the ZN-model with an energy  $\approx 2.5$  eV ( $\Gamma$  point) we arrive at a set of one- and two-center excitons generated by  $d-p_\sigma$  charge transfer, and occupying a very broad energy range from  $\approx 2$  up to  $\approx 13$  eV. The EELS data shows a double-peak structure of the CT gap which is determined by nearly degenerate intra-center and inter-center excitons.

The research was supported by a grant of the Ministry of Science and Art of Saxony (SMWK). The work in Ural State University was supported in part by Award No. REC-005 of the U.S. Civilian Research and Development Foundation for the Independent States of the Former Soviet Union (CRDF), Russian Ministry of Education, Grant No. E00-3.4-280, and Russian Foundation for Basic Researches, Grant No. 01-02-96404. We also acknowledge support by the Deutsche Forschungsgemeinschaft (DFG), project 436 UKR 113/49/0-1.

<sup>1</sup>J. Zaanen, G.A. Sawatzky, and J.W. Allen, Phys. Rev. Lett. **55**, 418 (1985).

<sup>2</sup>B.O. Wells, Z.-X. Shen, A. Matsuura, D.M. King, M.A. Kastner, M. Greven, and R.J. Birgeneau, Phys. Rev. Lett. **74**, 964 (1995).

<sup>3</sup>Y.Y. Wang, F.C. Zhang, V.P. Dravid, K.K. Ng, M.V. Klein, S.E. Schnatterly, and L.L. Miller, Phys. Rev. Lett. **77**, 1809 (1996).

<sup>4</sup>F.C. Zhang and K.K. Ng, Phys. Rev. B **58**, 13 520 (1998).

<sup>5</sup>J. Fink, M. Knupfer, S. Atzkern, and M.S. Golden, J. Electron Spectrosc. Relat. Phenom. **117-118**, 287 (2001).

<sup>6</sup>J. Fink, Adv. Electron. Electron Phys. **75**, 121 (1989).

<sup>7</sup>M.S. Hybertsen, E.B. Stechel, M. Schluter, and D.R. Jennison, Phys. Rev. B **41**, 11 068 (1990).

<sup>8</sup>R. Hayn, H. Rosner, V.Y. Yushankhai, S. Haffner, C. Dürr, M. Knupfer, G. Krabbes, M.S. Golden, J. Fink, H. Eschrig, D.J. Singh, N.T. Hien, A.A. Menovsky, C. Jung, and G. Reichardt, Phys. Rev. B **60**, 645 (1999).

<sup>9</sup>A.S. Moskvina, S.-L. Drechsler, R. Hayn, J. Malek, E.N. Kondrashov, and V.I. Cherepanov, (unpublished).

<sup>10</sup>J.J.M. Pothuizen, R. Eder, N.T. Hien, M. Matoba, A.A. Menovsky, and G.A. Sawatzky, Phys. Rev. Lett. **78**, 717 (1997).

<sup>11</sup>R. Neudert, Ph.D. thesis, University of Technology Dresden, 1999.

<sup>12</sup>R. Neudert, M. Knupfer, M.S. Golden, J. Fink, W. Stephan, K. Penc, N. Motoyama, H. Eisaki, and S. Uchida, Phys. Rev. Lett. **81**, 657 (1998).

<sup>13</sup>J.P. Falck, A. Levy, M.A. Kastner, and R.J. Birgeneau, Phys. Rev. Lett. **69**, 1109 (1992).

<sup>14</sup>S.L. Cooper, D. Reznik, A. Kotz, M.A. Karlow, R. Liu, M.V. Klein, W.C. Lee, J. Giapintzakis, D.M. Ginsberg, B.W. Veal, and A.P. Paulikas, Phys. Rev. B **47**, 8233 (1993).

<sup>15</sup>B.B. Krichevstov, R.V. Pisarev, A. Burau, H.-J. Weber, S.N. Barilo, and D.I. Zhigunov, J. Phys.: Condens. Matter **6**, 4795 (1994).